Vol. 03, Iss. 2 (2025) 266-272, DOI: 10.61552/JME.2025.02.011

Journal of Materials and Engineering

www.jme.aspur.rs

Research article

Natural Frequencies of FGP Sandwich Plates Resting on an Elastic Foundation Using HSDT: A Mini Study

Lan Hoang That Ton[a,*]

[a]*Faculty of Civil Engineering, University of Architecture, HCM city, Vietnam.*

Keywords:

Sandwich plate
FGP
Finite element analysis
HSDT
Elastic foundation

* Corresponding author:

Lan Hoang That Ton
E-mail: tonthathoanglan.247@gmail.com

Received: 29 October 2024
Revised: 24 November 2024
Accepted: 20 December 2024

A B S T R A C T

In this paper, the natural frequencies of functionally graded porous (FGP) sandwich plates laid on an elastic foundations are achieved using the C^0 type of a higher-order shear deformation theory (HSDT) and finite element model. This structure comprises a homogeneous metal bottom layer, a completely ceramic top layer, and an FGP core. These results related to this procedure are given using the Matlab software to verify the potential for use and contrasted with those of previous studies in the literature. Additionally, the effects of a number of parameters on the natural frequencies are provided.

1. INTRODUCTION

A team of Japanese scientists developed very advantageous functionally graded materials (FGM) in 1984. Following that, these smart materials were used much more frequently. This material offered a continuous variation of properties from the top surface to the bottom surface and was composed of a metal and ceramic blend. There are now more applications in fields like nuclear power plants, defense engineering, aerospace and submarine engineering, etc. An unavoidable extension is the sandwich plate structure with the FGM layer. Here are some studies related to this structure in the past few years. The work [1] was emphasized towards the development of models for the porosity occurring in the functionally graded structures. The porosities were modeled across the thickness for the functionally graded plate as well as for the functionally graded core of the sandwich plate, considering three different types of porosity distribution, i.e., symmetric center enhanced, top enhanced, and bottom enhanced. The influence of the porosities on the material properties was examined, and the properties were evaluated in view of porosities. Further, the influence of the porosities on the static behavior of functionally graded and functionally graded sandwich plates was investigated quantitatively, wherein the considered structures were modeled in the framework of an inverse hyperbolic shear deformation theory. The governing equations were obtained through the principle of virtual work, considering linear structural kinematics and generalized Hooke's law. These equations were solved in the closed form for the simply supported boundary conditions, and the response was obtained. In the article [2], the artificial neural network technique was used to examine how geometric discontinuities affected the vibrational response of porous sandwich functionally graded material plates with double functionally graded material facesheets. Generalized governing equations for the sandwich functionally graded material plate had been derived based on nonpolynomial-based higher-order shear deformation theory. Geometric discontinuities had been incorporated in terms of cut-outs in the sandwich functionally graded material plates. The functionally graded material layers integrated a porosity model, while the core layer was considered a ceramic layer within the sandwich functionally graded material plate structure. Additionally, the results were achieved using a C^0 continuous isoparametric finite element formulation with a four-noded, isoparametric quadrilateral element with seven degrees of freedom per node. A functionally graded porous sandwich plate reinforced with graphene platelets interacting with subsonic airflow on an elastic foundation was examined for nonlinear vibration and stability in the paper [3]. The plate was made up of two metal face layers and a functionally graded porous core reinforced with graphene platelets. The assumed modes method was used to export and discretize the nonlinear equation of the plate into ordinary equations based on Hamilton's principle. Via the computation of the system characteristic values, the impact of porosity, graphene platelet weight fraction, surface thickness ratio, and Winkler-Pasternak elastic foundation arguments on the critical divergence velocity of the plate under subsonic flow was demonstrated. A thorough analysis of the impact of these parameters on the system's nonlinear resonance behavior was made possible by the use of the Matcont toolbox to create nonlinear amplitude frequency resonance curves. The study [4] dealt with the free vibration analysis of skew sandwich plates. The sandwich plate was made up of three layers, with pure metal for the faces and metal foam for the core layer. The distribution of pores in the core was assumed to follow various functionally graded patterns. The governing equations of the plate were obtained by means of the first-order shear deformation theory. An oblique coordinate system was also defined, and the basic governing equations were transformed from the orthogonal system to the oblique one. The governing equations' matrix representation was established and an eigenvalue problem was extracted using the general concept of the Ritz method, in which the shape functions were constructed using the Chebyshev polynomials. In [5], a refined quasi-3D shear and normal deformation theory was used to bend a novel model of functionally graded sandwich plates, introducing an improved porosity distribution. The sandwich plates were lying on Pasternak's elastic foundation and exposed to sinusoidal mechanical loads. The shear correction factor was not required because both the shear and normal strains were taken into account. Depending on a specific function, the material properties of the sandwich plates varied continuously across the thickness direction. The equilibrium equations could be derived using the virtual work principle and solved using Navier's method. The paper [6] used Kirchhoff's hypothesis and the principle of virtual displacement to examine the static, stability, and free vibration behavior of multi-layer multi-directional functionally graded sandwich thin rectangular plates subjected to thermo-mechanical loadings. Effects of varying the physical properties through the thickness, length, and width directions and different boundary conditions were considered. Using the power law, exponential, and sigmoidal law functions, the rule of mixture was used to determine the temperature-position-dependent physical properties. Based on the constructed sandwich plate model, the dynamic properties of functionally graded porous sandwich plates with a square-celled core filled with viscoelastic material were examined in [7]. The first-order shear deformation theory, the equivalent theory of material mechanics, the virtual spring technology, the modified Fourier-Ritz method, and the Newmark-Beta approach were all combined to create the dynamic model. The static, free vibration, and buckling analysis of the simply supported functionally graded sandwich plates on elastic foundation were investigated using a hyperbolic shear and normal deformation plate theory, which was introduced in [8]. The theory accounted for the realistic variations of the displacements through the thickness. In the analysis, two common types of functionally graded sandwich plates, namely, homogeneous face sheets with functionally graded core and functionally graded face sheets with homogeneous core, were considered. The elastic foundation was described by the Pasternak model. The equations of motion were derived from Hamilton's principle. The closed-form solutions were obtained by using the Navier technique. The [9] provided an other finite-element procedure based on Reddy's third-order shear deformation plate theory to establish the motion equation of functionally graded porous sandwich plates resting on Kerr foundation, etc.

Returning to this study, the HSDT with C^0 form finite element method for FGP sandwich plates resting on an elastic foundation is shown. Recently, Shi successfully formulated a novel, improved yet simple third-order shear deformation plate theory based on rigorous kinematics of displacements, applied to the analysis of plates [10-12]. More specifically, the novelty here is the attempt to extend Matlab code based on Shi theory for the free vibration analysis to FGP sanwich plates lying on an elastic foundation, taking into account the influence of porosity in the core layer. This paper's subsequent sections are as follows: Part 2 provides information on the concept of material, changes in material properties, and the frequency analysis process. Part 3 displays the numerical results, and the final section offers some remarks.

2. FORMULATION

Figure 1 shows a plot of a FGP sandwich plate resting on an elastic foundation. The z-axis is perpendicular to the xy-plane, which is the plate's mid-plane. Additionally, this structure comprises a homogeneous metal bottom layer, a completely ceramic top layer, and an FGP core.

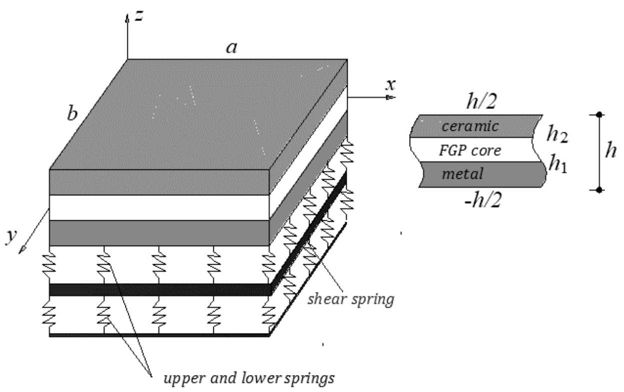

a) 3D illustration b) cross section

Fig. 1. The functionally graded sandwich plate with ceramic/metal face sheets and FGP core.

The ceramic volume fraction and metal volume fraction:

$$\begin{cases} V_c^b(z) = 0 & -h/2 \le z \le h_1 \\ V_c^c(z) = \left(\dfrac{z-h_1}{h_2-h_1}\right)^n \text{ with } & \begin{matrix} h_1 < z < h_2 \\ V_m^c(z) = 1 - V_c^c(z) \end{matrix} \\ V_c^t(z) = 1 & h_2 \le z \le h/2 \end{cases} \quad (1)$$

For core layer, the material properties $M^c(z)$ are provided:

$$M^c(z) = \left[M_m^c + \left(M_c^c - M_m^c\right)V_c^c\right] \times \times\left(1 - e_0 \cos\left(\frac{\pi z}{h}\right)\right) \quad (2)$$

Three digits, such as "t_1 / t_2 / t_3," indicate the ratio of the thicknesses of the top, bottom, and core layers. $h.t_1 / (t_1 + t_2 + t_3)$ represents the bottom skin, $h.t_2 / (t_1 + t_2 + t_3)$ represents the core layer, and $h.t_3 / (t_1 + t_2 + t_3)$ represents the top skin. Besides, an elastic foundation with an upper layer k_u, a shear layer k_s, and a lower layer k_l can be determined as

$$\Xi = \frac{k_l k_u}{k_l + k_u} w - \frac{k_s k_u}{k_s + k_u}\left[\left(\frac{\partial w}{\partial x}\right)^2 + \left(\frac{\partial w}{\partial y}\right)^2\right] \quad (3)$$

On the other hand, with two additional variables added, the displacement field can be expressed in terms of C^0-HSDT based on Shi's theory and a slight modification [11]. To compute a low-order quadrilateral element with four nodes, all that is needed is the first derivative of transverse displacement. The unknown variables are currently shown as

$$u(x,y,z) = u_0 + \left(\frac{1}{4}z - \frac{5}{3h^2}z^3\right)\phi_x^b + + \frac{5}{4}\left(z - \frac{4}{3h^2}z^3\right)\phi_x^s \quad (4)$$

$$v(x,y,z) = v_0 + \left(\frac{1}{4}z - \frac{5}{3h^2}z^3\right)\phi_y^b + + \frac{5}{4}\left(z - \frac{4}{3h^2}z^3\right)\phi_y^s \quad (5)$$

$$w(x,y,z) = w_0 \quad (6)$$

With these seven unknowns, three displacements and four rotations due to the bending and shear effects, the displacement-strain relations can be written in matrix form.

$$\varepsilon = \begin{Bmatrix} u_{0,x} \\ v_{0,y} \\ u_{0,y} + v_{0,x} \end{Bmatrix} + \\ +z\frac{1}{4}\begin{Bmatrix} \left(5\phi^s_{x,x} + \phi^b_{x,x}\right) \\ \left(5\phi^s_{y,y} + \phi^b_{y,y}\right) \\ \left(5\phi^s_{x,y} + 5\phi^s_{y,x} + \phi^b_{x,y} + \phi^b_{y,x}\right) \end{Bmatrix} + \\ +z^3\frac{-5}{3h^2}\begin{Bmatrix} \phi^s_{x,x} + \phi^b_{x,x} \\ \phi^s_{y,y} + \phi^b_{y,y} \\ \phi^s_{x,y} + \phi^b_{x,y} + \phi^s_{y,x} + \phi^b_{y,x} \end{Bmatrix} \tag{7}$$

$$\gamma = \begin{Bmatrix} \frac{5}{4}\phi^s_y + \frac{1}{4}\phi^b_y + w_{,y} \\ \frac{5}{4}\phi^s_x + \frac{1}{4}\phi^b_x + w_{,x} \end{Bmatrix} + z^2\frac{-5}{h^2}\begin{Bmatrix} \phi^s_y + \phi^b_y \\ \phi^s_x + \phi^b_x \end{Bmatrix} \tag{8}$$

The constitutive equation is expressed

$$\sigma = D_m(z)\varepsilon \quad \text{and} \quad \tau = D_s(z)\gamma \tag{9}$$

in which

$$\sigma = \begin{bmatrix} \sigma_x & \sigma_y & \sigma_{xy} \end{bmatrix}^T; \ \tau = \begin{bmatrix} \tau_{yz} & \tau_{xz} \end{bmatrix}^T \tag{10}$$

$$D_m(z) = \frac{E(z)}{1-\nu(z)^2}\begin{bmatrix} 1 & \nu(z) & 0 \\ \nu(z) & 1 & 0 \\ 0 & 0 & (1-\nu(z))/2 \end{bmatrix}; \\ D_s(z) = \frac{E(z)}{2(1+\nu(z))}\begin{bmatrix} 1 & 0 \\ 0 & 1 \end{bmatrix} \tag{11}$$

The generalized displacements can hence be approximated as

$$u_0 = Nq_e \tag{12}$$

with

$$u_0 = \begin{bmatrix} u_0 & v_0 & w & \phi^s_x & \phi^s_y & \phi^b_x & \phi^b_y \end{bmatrix}^T; \\ N = \begin{bmatrix} N_1 & N_2 & N_3 & N_4 \end{bmatrix}; \\ q_e = \begin{bmatrix} q_{1e} & q_{2e} & q_{3e} & q_{4e} \end{bmatrix}^T \tag{13}$$

q_e and N are the unknown displacement vector and the shape function vector. The strain can be rewritten

$$\left(B_1 + B_2 + B_3\right)q_e = \varepsilon \tag{14}$$

$$\left(B_4 + B_5\right)q_e = \gamma \tag{15}$$

in which

$$B_1 = \sum_{i=1}^{4}\begin{bmatrix} N_{i,x} & 0 & 0 & 0 & 0 & 0 & 0 \\ 0 & N_{i,y} & 0 & 0 & 0 & 0 & 0 \\ N_{i,y} & N_{i,x} & 0 & 0 & 0 & 0 & 0 \end{bmatrix}; \\ B_2 = \\ \frac{1}{4}\sum_{i=1}^{4}\begin{bmatrix} 0 & 0 & 0 & 5N_{i,x} & 0 & N_{i,x} & 0 \\ 0 & 0 & 0 & 0 & 5N_{i,y} & 0 & N_{i,y} \\ 0 & 0 & 0 & 5N_{i,y} & 5N_{i,x} & N_{i,y} & N_{i,x} \end{bmatrix} \tag{16}$$

$$B_3 = -\frac{5}{3h^2}\times \\ \times\sum_{i=1}^{4}\begin{bmatrix} 0 & 0 & 0 & N_{i,x} & 0 & N_{i,x} & 0 \\ 0 & 0 & 0 & 0 & N_{i,y} & 0 & N_{i,y} \\ 0 & 0 & 0 & N_{i,y} & N_{i,x} & N_{i,y} & N_{i,x} \end{bmatrix} \tag{17}$$

$$B_4 = \sum_{i=1}^{4}\begin{bmatrix} 0 & 0 & N_{i,y} & 0 & \frac{5}{4} & 0 & \frac{1}{4} \\ 0 & 0 & N_{i,x} & \frac{5}{4} & 0 & \frac{1}{4} & 0 \end{bmatrix}; \\ B_5 = -\frac{5}{h^2}\sum_{i=1}^{4}\begin{bmatrix} 0 & 0 & 0 & 0 & 1 & 0 & 1 \\ 0 & 0 & 0 & 1 & 0 & 1 & 0 \end{bmatrix} \tag{18}$$

The components of forces and moments can be introduced

$$\bar{N} = \bar{A}\varepsilon^{(0)} + \bar{B}\varepsilon^{(1)} + \bar{E}\varepsilon^{(3)}; \\ \bar{M} = \bar{B}\varepsilon^{(0)} + \bar{D}\varepsilon^{(1)} + \bar{F}\varepsilon^{(3)}; \\ \bar{P} = \bar{E}\varepsilon^{(0)} + \bar{F}\varepsilon^{(1)} + \bar{H}\varepsilon^{(3)}; \\ \bar{Q} = \hat{A}\gamma^{(0)} + \hat{B}\gamma^{(2)}; \\ \bar{R} = \hat{B}\gamma^{(0)} + \hat{D}\gamma^{(2)} \tag{19}$$

with

$$\bar{A} = \int_{-h/2}^{h/2} D_m(z)dz, \quad \bar{B} = \int_{-h/2}^{h/2} zD_m(z)dz \\ \bar{D} = \int_{-h/2}^{h/2} z^2 D_m(z)dz \tag{20}$$

$$\bar{E} = \int_{-h/2}^{h/2} z^3 D_m(z)dz, \quad \bar{F} = \int_{-h/2}^{h/2} z^4 D_m(z)dz \\ \bar{H} = \int_{-h/2}^{h/2} z^6 D_m(z)dz \tag{21}$$

$$\hat{A} = \int_{-h/2}^{h/2} D_s(z)dz, \quad \hat{B} = \int_{-h/2}^{h/2} z^2 D_s(z)dz \\ \hat{D} = \int_{-h/2}^{h/2} z^4 D_s(z)dz \tag{22}$$

The stiffness matrix of element with two parts is presented

$$K_e = \int_{S_e} \begin{Bmatrix} B_1 \\ B_2 \\ B_3 \\ B_4 \\ B_5 \end{Bmatrix}^T \begin{bmatrix} \bar{A} & \bar{B} & \bar{D} & 0 & 0 \\ \bar{B} & \bar{E} & \bar{F} & 0 & 0 \\ \bar{D} & \bar{F} & \bar{H} & 0 & 0 \\ 0 & 0 & 0 & \hat{A} & \hat{B} \\ 0 & 0 & 0 & \hat{B} & \hat{D} \end{bmatrix} \begin{Bmatrix} B_1 \\ B_2 \\ B_3 \\ B_4 \\ B_5 \end{Bmatrix} dS \quad (23)$$

$$K_e^{foundation} = \frac{k_l k_u}{k_l + k_u} \int_{S_e} N_f^T N_f dS - \frac{k_s k_u}{k_s + k_u} \int_{S_e} \begin{bmatrix} \left(\frac{\partial N_f}{\partial x}\right)^T \left(\frac{\partial N_f}{\partial x}\right) + \\ + \left(\frac{\partial N_f}{\partial y}\right)^T \left(\frac{\partial N_f}{\partial y}\right) \end{bmatrix} dS \quad (24)$$

in which

$$N_f = \sum_{i=1}^{4} \begin{bmatrix} 0 & 0 & N_i & 0 & 0 & 0 & 0 \end{bmatrix} \quad (25)$$

The mass matrix of element is given

$$M_e = \int_{V_e} N^T L^T \rho(z) L N dV = \int_{S_e} N^T \left(\int_{-h/2}^{h/2} \rho(z) L^T L dz \right) N dS \quad (26)$$

with

$$L = \begin{bmatrix} 1 & 0 & \left(\frac{1}{4}z - \frac{5}{3h^2}z^3\right)\frac{\partial}{\partial x} & \frac{5}{4}\left(z - \frac{4}{3h^2}z^3\right) & 0 \\ 0 & 1 & \left(\frac{1}{4}z - \frac{5}{3h^2}z^3\right)\frac{\partial}{\partial y} & 0 & \frac{5}{4}\left(z - \frac{4}{3h^2}z^3\right) \\ 0 & 0 & 1 & 0 & 0 \end{bmatrix} \quad (27)$$

The frequency equation can be solved by

$$\left(K - \omega^2 M\right) d = 0 \quad (28)$$

3. NUMERICAL SOLUTIONS

To verify the application of this procedure, a FGP sandwich plate with the material properties as in Table 1 is considered. Using these material parameters, Table 2 shows the first dimensionless frequencies $\bar{\omega} = \omega \frac{a^2}{\pi^2} \sqrt{\frac{\rho_c h}{D_c}}$ with $D_c = \frac{E_c h^3}{12\left(1 - \nu_c^2\right)}$ of (CSSC) FGP square sandwich plates with thickness $h = a/75$ and foundation parameters $k_l = k_u = 75$, $k_s = 20$. Besides, the mesh 20 x 20 is used in this paper.

As can be observed, the results obtained are in good agreement with [9]. Figure 2 shows the first four mode shapes of this structure with the ratio of thickness 1/1/1 and changing boundary condition from (CSSC) to (SSSS).

Table 1. The material properties.

SUS304	E_m = 201.04 GPa, ν_m = 0.3, ρ_m= 8166 kg/m^3
Si_3N_4	E_c = 348.43 GPa, ν_c = 0.3, ρ_c= 2370 kg/m^3
Al	E_m = 70 GPa, ν_m = 0.3, ρ_m= 2707 kg/m^3
Al_2O_3	E_c = 380 GPa, ν_c = 0.3, ρ_c= 3800 kg/m^3

Table 2. The comparison of the first dimensionless frequency of FGP square sandwich plate.

Ratio of thicknesses	e_0	*n*					
		0		1.5		4.5	
		[9]	present	[9]	present	[9]	present
1/1/1	0	2.8541	2.7299	2.8292	2.6776	2.8343	2.6914
	0.2	2.9242	2.7944	2.8979	2.7612	2.9017	2.7737
	0.5	3.0375	2.9467	3.0114	2.9258	3.0134	2.9309
1/4/1	0	3.0771	2.9697	2.8771	2.9134	2.8816	2.9184
	0.2	3.2076	3.1104	3.0109	2.9746	3.0167	2.9797
	0.5	3.4624	3.5321	3.2661	3.3367	3.2730	3.3401
2/2/1	0	2.8178	2.6915	2.8547	2.8015	2.8859	2.8484
	0.2	2.9111	2.7884	2.9451	2.8449	2.9739	2.8991
	0.5	3.0729	3.1006	3.1000	3.1227	3.1237	3.2169

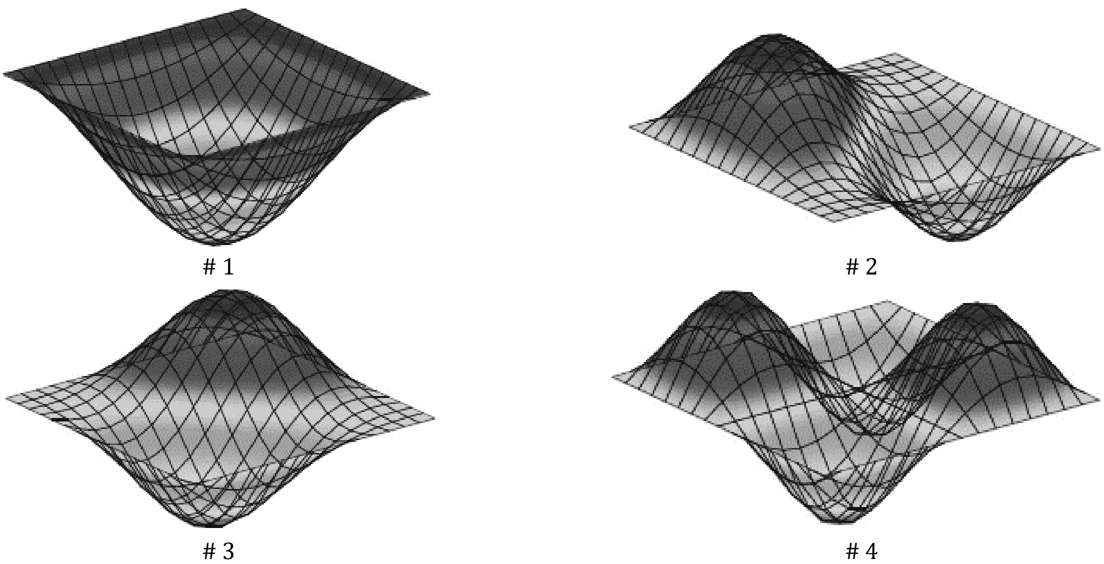

Fig. 2. The first four mode shapes for FGP sandwich square plate with ratio of the thicknesses 1/1/1, n = 1.5, e_0 = 0.1 and (*SSSS*) boundary condition.

Table 3. The first four dimensionless frequencies of FGP square sandwich plate.

Ratio of thicknesses	$\bar{\omega}_1$	$\bar{\omega}_2$	$\bar{\omega}_3$	$\bar{\omega}_4$
	SSSS ($h = a/10$)			
1/1/1	2.5119	4.4469	4.4512	4.7822
1/2/1	2.6126	4.5027	4.5385	4.8291
1/6/1	2.7308	4.6221	4.6694	4.9148
CCCC ($h = a/100$)				
1/1/1	3.4713	6.2188	6.2278	8.6633
1/2/1	3.5844	6.4173	6.4193	8.9204
1/6/1	3.7022	6.6207	6.6279	9.1556

Finally, Table 3 presents the first four dimensionless frequencies of FGP square sandwich plates via different ratio of thicknesses with material properties n = 5; e_0 = 0.4. From these results, it can be concluded that increasing the FGP core thickness results in an increase in the dimensionless frequencies.

4. CONCLUSION

Using this recommended element in the numerical modeling has some benefits within the context of the C^0-HSDT model. Successfully applied to the analysis of FGP sandwich plates resting on an elastic foundation and provided results without needing shear-correct factors. It is additionally pointed out that this model does not require a large computing cost and just makes use of bilinear function approximations. Additionally, numerical examples show that this element does not display the hourglass phenomenon and yields satisfactory results when compared to other published solutions from previous studies. Finally, this element type may soon be expanded to include nonlinear vibration analysis of plate structures lying on elastic foundations.

REFERENCES

[1] H. Singh, G. Bhardwaj, and N. Grover, "Modeling and static analysis of porous functionally graded and FG-sandwich plates," *Struct.*, vol. 68, p. 107034, 2024, doi: 10.1016/j.istruc.2024.107034.

[2] D. Singh, S. Rai, and A. Gupta, "Vibration analysis of sandwich functionally graded material plate with cut-outs using artificial neural network technique," *Thin Wall Struct.*, vol. 202, p. 112072, 2024, doi: 10.1016/j.tws.2024.112072.

[3] Z. Wang and G. Yao, "Nonlinear vibration and stability of sandwich functionally graded porous plates reinforced with graphene platelets in subsonic flow on elastic foundation," *Thin Wall Struct.*, vol. 194, p. 111327, 2024, doi: 10.1016/j.tws.2023.111327.

[4] J. Zhu, Z. Fang, X. Liu, J. Zhang, and Y. Kiani, "Vibration characteristics of skew sandwich plates with functionally graded metal foam core," *Struct.*, vol. 55, pp. 370–378, 2023, doi: 10.1016/j.istruc.2023.06.039.

[5] A. M. Zenkour and R. A. Alghanmi, "A refined quasi-3D theory for the bending of functionally graded porous sandwich plates resting on elastic foundations," *Thin Wall Struct.*, vol. 181, p. 110047, 2022, doi: 10.1016/j.tws.2022.110047.

[6] S. Rajasekaran, H. B. Khaniki, and M. H. Ghayesh, "Thermo-mechanics of multi-directional functionally graded elastic sandwich plates," *Thin Wall Struct.*, vol. 176, p. 109266, 2022, doi: 10.1016/j.tws.2022.109266.

[7] Z. Gao, H. Li, J. Zhao, J. Guan, and Q. Wang, "Analyses of dynamic characteristics of functionally graded porous (FGP) sandwich plates with viscoelastic materials-filled square-celled core," *Eng. Struct.*, vol. 248, p. 113242, 2021, doi: 10.1016/j.engstruct.2021.113242

[8] S. S. Akavci, "Mechanical behavior of functionally graded sandwich plates on elastic foundation," *Compos. Part B-Eng.*, vol. 96, pp. 136–152, 2016, doi: 10.1016/j.compositesb.2016.04.035

[9] N. T. Do, T. T. Tran, and Q. H. Pham, "A new finite-element procedure for vibration analysis of FGP sandwich plates resting on Kerr foundation," *Curved Layer. Struct.*, vol. 10, p. 20220195, 2023, doi: 10.1515/cls-2022-0195.

[10] L. H. T. That, "Four-node quadrilateral C0-element based on cell-based smoothed strains strategy and third-order shear deformation theory for functionally graded carbon nanotube reinforced composite plates," *Rakenteiden Mekaniikka*, vol. 56, no. 1, pp. 1–23, 2023, doi: 10.23998/rm.119608.

[11] [H. L. Ton-That, "Finite element analysis of functionally graded skew plates in thermal environment based on the new third-order shear deformation theory," *J. Appl. Comput. Mech.*, vol. 6, pp. 1044–1057, 2020, doi: 10.22055/jacm.2019.31508.1881.

[12] T. Q. Bui et al., "On the high temperature mechanical behaviors analysis of heated functionally graded plates using FEM and a new third-order shear deformation plate theory," *Compos. Part B-Eng.*, vol. 92, pp. 218–241, 2016, doi: 10.1016/j.compositesb.2016.02.048.